Rainfall-Induced Landslide Early Warning System based on corrected mesoscale numerical models: an application for the Southern Andes

Ivo Fustos[1], Nataly Manque[2], Daniel Vásquez[1,3], Mauricio Hermosilla[1], Viviana Letelier[1]

[1]Department of Civil Engineering, University of La Frontera, Temuco, Chile
[2]Universidad Adolfo Ibáñez, Santiago, Chile
[3]Master on Engineering Sciences, University of La Frontera, Temuco, Chile

Correspondence to: Ivo Fustos (ivo.fustos@ufrontera.cl)

Abstract. Rainfall-Induced Landslide Early Warning Systems (RILEWS) are critical tools for reducing and mitigating economic and social damages related to landslides. Despite this utility, the Southern Andes do not have an operational-scale RILEWS yet. In this contribution, we present a pre-operational RILEWS based on the Weather and Research Forecast (WRF) model and geomorphological features coupled to logistic models in the Southern Andes. The models have been forced using simulations of precipitation. We correct the precipitation derived from WRF using 12 weather stations through a bias correction approach. The models were trained using 57 well-characterized Rainfall-Induced Landslides (RIL) and validated by ROC analysis. We show that WRF does not represent the spatial variability of the precipitation. Therefore, accurate precipitation needs a bias correction in the study zone. Accurate precipitation simulations allow RILEWS with high predicting capacity (area under the curve, AUC of 0.80) using daily precipitation data and slope. We conclude that our proposal is suitable at an operational level. The proposed RILEWS will become a support in the mitigation of RIL events related to climate change.

1 Introduction

Rainfall Induced Landslide Early Warning Systems (RILEWS) become a powerful alternative for mitigating human losses and reducing infrastructure damages (Guzzetti et al., 2020; Chikalamo et al., 2020; Hermle et al., 2021). The increase of Rainfall-Induced Landslides (RIL) events showed devastating effects, including loss of human life and destruction of the natural and urban environment (Marjanovi? et al., 2018). Recent RIL affected critical infrastructure and highways in populated areas (Chikalamo et al., 2020; Fustos et al., 2020a; Peruccacci et al., 2017; Fustos et al., 2021). In South America, RIL has caused high social and economic impacts; they require better evaluation in future (Sepulveda & Petley, 2015). The present work evaluates the design of a RILEWS using a mesoscale atmospheric model coupled to a logistic model to mitigate the effect of RIL in the Southern Andes.

Due to new extreme rainfall events related to climate change, RIL events are increasing in the Southern Andes and other parts of the world. To mitigate the impact of extreme precipitation RILEWS have gained interest to mitigate the impact of RIL using different approaches (Peres & Cancelliere, 2014; Tiranti et al., 2014; Sättele et al., 2015; Segoni et al., 2018;

Cremonini and Tiranti, 2018; Fan et al., 2019; Tiranti et al., 2019; Thirugnanam et al., 2020; Bernard and Gregoretti, 2021; Lee et al., 2021). RILEWS based on precipitation thresholds shows good agreement but do not consider the effect of soil moisture, leading to bias in their predictive capacity (Marra et al., 2017; Zhao et al., 2019; Chikalamo et al., 2020). Some historical-based RILEWS with long-term observations, climate reanalysis models and atmospheric mesoscale models experiment issues related to the spatial and temporal resolution reducing the performance due to low precipitation accuracy (Lazzari & Piccarreta, 2018; Tichavský et al., 2019).

RILEWS requires accurate precipitation data delivered from local weather stations in dense weather networks, satellite estimations and atmospheric mesoscale models. However, atmospheric mesoscale models showed incapable of representing accurate precipitation fields in areas with complex topography like the Southern Andes (Yáñez-Morroni et al., 2018). Currently, mesoscale models are restricted to the quality of their atmospheric forcings, needing to generate ensembles to obtain approximate solutions (Wayand et al., 2013). Moreover, the mesoscale models demand intensive computational efforts that increase the difficulty of coupling to RILEWS (Yáñez-Morroni et al., 2018; Schumacher et al., 2020; Yang et al., 2021). Recently, mesoscale atmospheric models coupled to local weather stations allow delimitating susceptible to RIL areas means deterministic numerical models (Fustos et al., 2020a). Nowadays, bias correction approaches contribute to reducing the time computing of mesoscale models, improving the estimation of precipitation using in-situ stations (Srivastava et al., 2015; Bannister et al., 2019; Heredia et al., 2018; Jeong & Lee, 2018; Osman et al., 2019; Worku et al., 2020). Therefore, a correct implementation of mesoscale models could allow accurate precipitation in RILEWS. Nonetheless, the application of corrected mesoscale models in RILEWS in complex topography has not been evaluated yet.

The object of the present work was to evaluate the implementation of a RILEWS based on mesoscale atmospheric model coupled to logistic model. We corrected mesoscale models (models that allow represent atmospheric process to synoptic-scale) using weather stations, generating RIL-prone probability zones for the first time in the Southern Andes. The paper is structured as follows: after the introduction, the second section describes the study site and its pertinence to implement RILEWS. In the third section, we describe the data and methods, including the calibration and validation procedures. In the fourth section, we outline the main results of the proposed RILEWS, focusing on the quality of predictors and model outputs. The fifth and final section comprises the discussion and conclusions, presenting the implications of this proposal and their general applicability to the southern Andes.

2 Study area

We evaluated the implementation of RILEWS in the Southern Andes and the northern part of the Patagonian Andes (~40.0° – 42.5°S, ~72.0° – 73.5° W, Figure 1). A prolonged increase of RIL events in this area took place during the period 2012-2019, generated by extreme precipitation events. The area presents three principal morphological units in bands oriented north-south. From west to east, they are the Coastal Range, the Central Valley and the Andes Range (Figure 1). In the western area, altitudes range from 100-1,000 m a.s.l., with slopes between 0 and 25°. In the central valley, the maximum

altitude is 150 masl, with slopes between 0 and 15° in the central part and between 25 and 45° towards the Andes. Finally, the highest altitudes (400 to 2,700 masl) and the steepest slopes (25 – 70°) are found in the eastern zone (Gomez-Cardenas & Garrido-Urzua, 2018).

Average annual precipitation is strongly correlated with topography and latitude. In the north segment (~40°33' – ~41°10' S) it is over 1,200 mm per year, while in the south (~41°10' – ~42°10' S) it rises to over 1,400 mm per year. In the Central Valley, the precipitation exceeds 1,910 mm per year. The highest precipitations are recorded in the Andes Range, of over 4,000 mm (Alvarez-Garreton et al., 2018). The climate in the area is classified as oceanic climate (Beck et al., 2018) with a dry summer in the north portion, but no dry months in the south (Alvarez-Garreton et al., 2018).

The oldest geological units in the area correspond to cretaceous intrusive bodies which emerge in the Rupanco lake peninsula and further south. In the Coastal Range, there are outcrops of metamorphic rocks from the Paleozoic Triassic (300-250 Ma). These rocks are largely covered by sedimentary deposits of various origins: marine from the Oligocene-Miocene (eastern flank of the Coastal Range), volcanic from the Oligocene-Miocene (40 to 5 Ma; south of Rupanco lake), and glacial from the Pleistocene-Holocene. In the SE of the region is the North Patagonian Batholith (132-77 Ma), consisting of granites, granodiorites, tonalites and leucogranites (Gomez-Cardenas & Garrido-Urzua, 2018). Elsewhere in the region, there are clayey soils called trumaos and ñadis, which have developed from glacial-fluvial-volcanic sediments. These soils present a high organic content, poor drainage and low development (Blanco & de la Balze, 2004).

Figure 1 Study area in the Southern Andes Zone and the northern part of the Patagonian Andes. RIL events in the area are highlighted in yellow dots and red stars mark the meteorological stations available. Hillshade based on SRTM data.

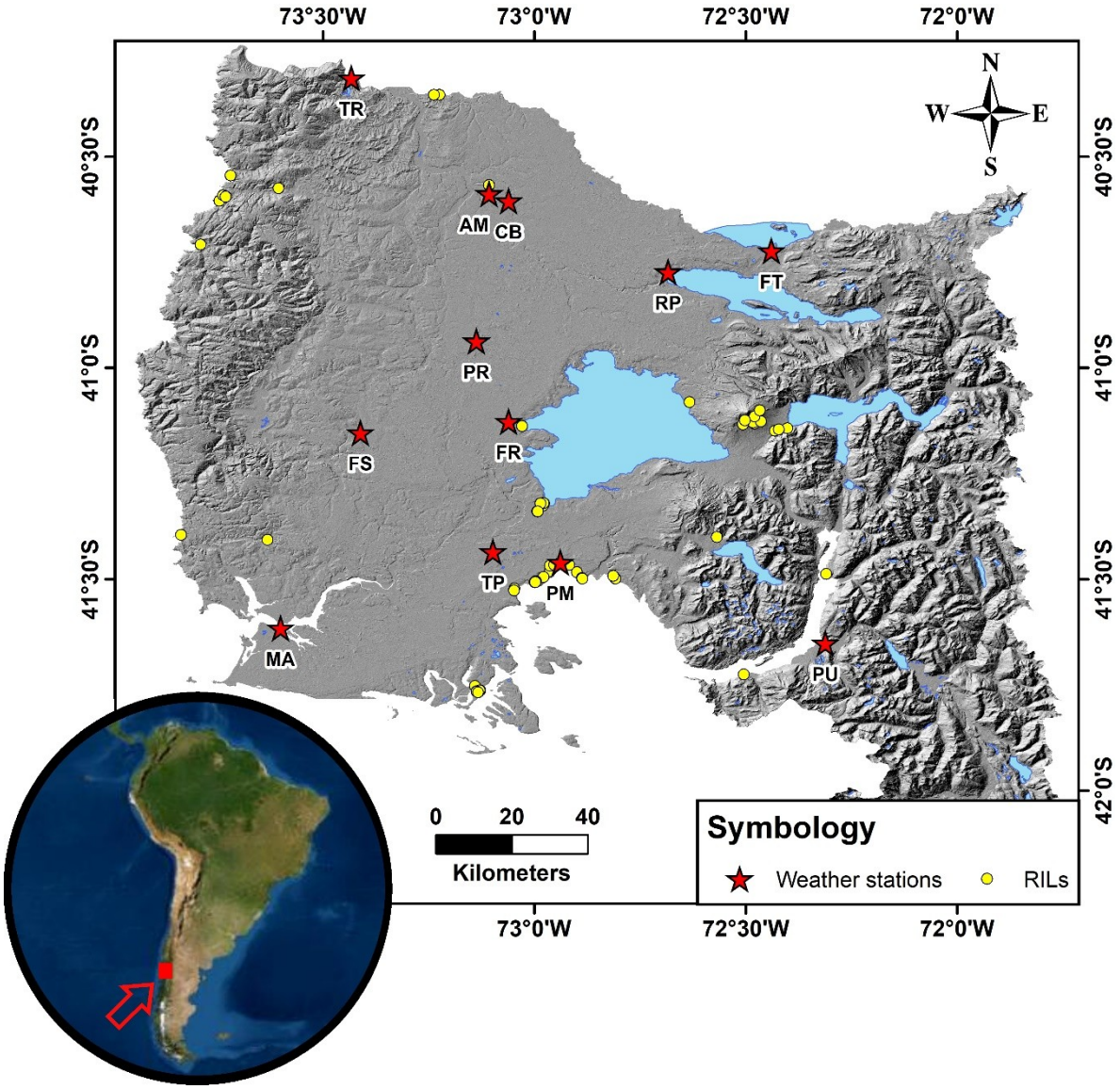

85

3 Methodology

We assessed the feasibility of a RILEWS applied to RIL using geomorphological and precipitation forcings for the Southern Andes. We consider an approximation of the probability of occurrence of RIL through logistic distributions. The probability allows a spatialization of "prone-landslide" or "not prone-landslide" conditions under established precipitation and topographical conditions. Precipitation data and local geomorphological features were integrated into a logistic model as predictors to evaluate the occurrence of RIL. These variables were taken into account because both the precipitation and the topography predispose the study area to RIL (Fustos et al., 2017; 2020a). We do not use additional data, such as soil moisture or climatic index, to avoid complex models allowing fast estimations into an operational stage. We used a RIL database (Gomez-Cardenas & Garrido-Urzua, 2018) being separated into calibration sub-database and validation sub-database to evaluate the models' performance.The bias associated with the precipitation obtained from the mesoscale model was corrected using in-situ stations (Figure 2). To establish the reliability of the model for the correct prediction of RIL, its sensitivity was calculated using the validation subset. This allowed the RIL prediction sensitivity to be characterised for operational implementation in future LEWS.

Figure 2 Short methodological description. The first phase explained in detail in section 3.1 and the second stage explained in sections 3.2 and 3.3.

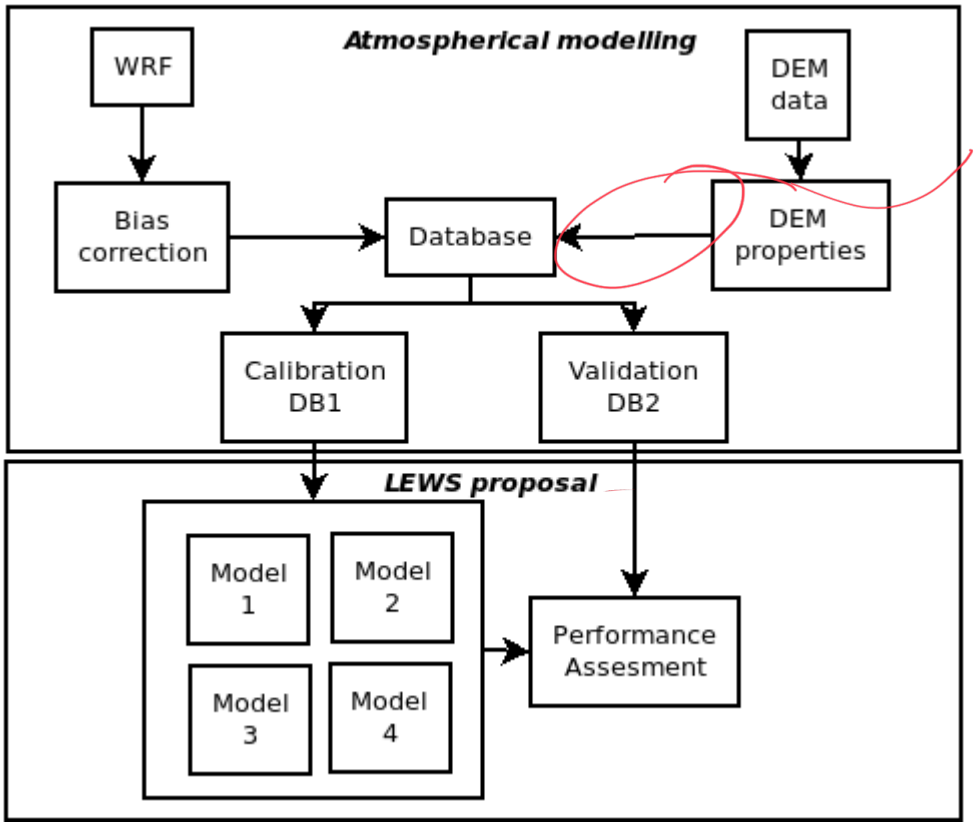

improve arrow (straight)

3.1 Atmospheric modelling

The study area contains a limited number of meteorological stations, becoming a challenge to represent the spatial distribution of precipitation. To overcome the limitation imposed by the meteorological data, precipitation fields were estimated using the Weather and Research Forecast model 4.0 (WRF, Skamarock et al., 2019). Atmospheric conditions were simulated for the period 2014 to 2018 at hourly time resolution. We used a spatial resolution of 4 km that allows representing the complex topography of the Andes. WRF parametrisation followed the WSM 3-Class Simple Ice Scheme microphysical model (Hong et al., 2004), while the soil-atmosphere interaction was parametrised by the Unified Noah Land-Surface Model (Tewari et al., 2004). Final Operational Global Analysis product from the US–National Centers for Environmental Prediction NCEP, also known as FNL (NCEP, 2000), was used as the global forcing to obtain the solutions of precipitation at 4-km or mesoscale (resolution to an order of kilometres).

The precipitation fields of the WRF model were compared with 12 meteorological stations available in the area to evaluate the bias of the numerical model (Figure 1). Biases associated with local effects of the parametrisation selected in WRF were corrected by MeteoLab (Wilcke, 2013) using three different methods (Table 1). We compared the methods with different

how were these 12 stations selected ? Are there other

statistics functions such as bias, MAE, RMSE, and Pearson and Spearman correlations. Subsequently, the model corrected with the lowest RMSE in precipitation was used in a RILEWS implementation.

Table 1: Correction methods applied, with references.

CORRECTION	REFERENCE
PP_M4A	Perfect prog approach. Reassessing model uncertainty for regional projections of precipitation with an ensemble of statistical downscaling methods (San-Martín et al., 2017).
ISI-MIP	A trend-preserving bias correction & ndash; The ISI-MIP approach (Hempel et al., 2013).
BC_QPQM	Bias correction approach. Precipitation bias correction methods for high-resolution regional climate simulations using COSMO-CLM: Effects on extreme values and climate change signal (Gutjahr and Heinemann, 2013).

3.2 Rainfall-Induced Landslide Early Warming

We propose a model for RILEWS based on the probability of occurrence of RIL in space and time. The probability was determined using Logit and Probit logistic distribution functions, which have been implemented previously in the Southern Andes (Fustos et al., 2017; 2020b). The advantage of logistic regressions is that they establish statistical relations between physical processes at different scales with a limited quantity of information (Fustos et al., 2020b). The logistic regressions were trained based on the local geomorphological conditions (slope) and previously modelled and corrected precipitation simulations.. We used slope values derived from SRTM data. A limited number of 4,987 RIL have been reported for the south of Chile (Gomez-Cardenas & Garrido-Urzua, 2018). However, 2.035 RIL exist in the zone, and only 57 RIL events have an exact date. The final database considers mudflow, debris flow and mass wasting. The actual database is not suitable to establish RILEWS using thresholds due to the scarce amount (Peres and Cancelliere, 2021). The current dataset is the most comprehensive landslide catalogue for the zone in comparison to well-validated global datasets such as Global Landslide Catalog (GLC) (Kirschbaum et al., 2010) and the Global Fatal Landslide Database (GFLD) (Froude and Petley, 2018) developed into other studies (Destro et al., 2017; Rossi et al., 2017; Wang et al., 2021).

The Logit distribution model fit the probability of occurrence of an event using a logistic curve (Li et al., 2011). The Logit distribution model (L) is given by:

$$L(y_i=1)=\frac{\exp\left(\beta_0^{'}+\sum_{k=1}^{N}\beta_k^{'}X_k\right)}{1+\exp\left(\beta_0^{'}+\sum_{\square}^{\square}\square_{\square}^{\square}\square_{\square}\left|\square_{\square}^{\square}\square_{\square}\right.\right)} \quad \textbf{(Eq. 1).}$$

where $L(y_i=1)$ is the probability of occurrence of a RIL, N is the number of predictors used (X_k), $\beta_k^{'}$ are the coefficients of the function and $\beta_0^{'}$ is the intercept. A Probit distribution also uses binary dependent variables and its main difference from the Logit distribution is the use of the inverse standard normal distribution. The Probit distribution (P) (McCullagh & Nelder, 1989; Javier & Velazquez, 1990) is given by:

$$P(y_i=1)=\Phi^{-1}\left(\beta_0+\sum_{k=1}^{N}\beta_k X_k+\varepsilon\right) \quad \textbf{(Eq. 2).}$$

where k, β and X_k refer to the same variables as the Logit distribution, ε is the error of the fit with standard normal distribution $\varepsilon \sim N(0,\Sigma)$ and Φ^{-1} denotes an inverse normal probability function (McCullagh & Nelder, 1989). Four predictors were used for both the Logit and Probit functions, daily precipitation, precipitation over the previous 7 and 30 days, and slope (Table 2).

The complete RIL database was split into a calibration sub-base (DB1) and an independent calibration validation sub-base (DB2) for subsequent evaluation (Figure 2). The database was split by taking from 20 to 30% of the data, chosen at random, for calibration. A calibration set was selected 100 times to obtain β_k and $\beta_k^{'}$, and their standard deviations denoted by σ_k and $\sigma_k^{'}$respectively, calculated according to the methodology presented by Fustos et al. (2020b).

Table 2: Models and predictors incorporated.

	Daily precipitation	**Seven-day accumulated precipitation**	**Thirty-day accumulated precipitation**	**Slope**
Model 1	Considered	-	-	Considered
Model 2	-	Considered	-	Considered
Model 3	-	-	Considered	Considered
Model 4	Considered	Considered	-	Considered

3.3 Performance assessment

The quality of each regression was evaluated by ROC analysis (Fawcett, 2006) using the independent database BD2 (Figure 2). The DB2 has georeferenced the initial failure zone. We compared the initial failure zone to the pixel of our models (pixel that includes the point). This allowed us to understand the degree of accuracy in identifying a RIL event under determined conditions of slope and precipitation. A probability threshold (tolerance) was established to define the instant when the

models identify a RIL event correctly. The tolerance was defined from the results of the ROC curve for probability thresholds between 50 and 95%. In this way, the sensitivity of each iteration was estimated (Eq. 3), representing the capacity of the set of estimators to detect RIL events correctly (Fawcett, 2006; Hand & Till, 2001). The sensitivity (S) was defined as the ratio of true positive predictions of events (TP), over the total of positive events (including false-negative predictions – FN). The specificity (E) was also calculated (Eq. 4) to evaluate the capacity of detection of non-RIL events or true negative (TN), to avoid false positives (FP) (Fawcett, 2006). Therefore, this methodology made it possible to evaluate the capacity of each model to detect RIL events (Fustos et al., 2020b). We propose that the threshold must be suitable to separate a prone-landslide event from a non-prone-landslide event. The threshold maximizes the sensibility in the four models with different degrees of performance of RILEWS.

$$S=TP/(TP+FN) \quad \textbf{(Eq. 3).}$$

$$E=TN/(TN+FP) \quad \textbf{(Eq. 4).}$$

4 Results

This work evaluated a new RILEWS based on two logistic models and forced by geomorphological and atmospheric conditions on a mesoscale in the Southern Andes. We analysed the quality of the representation of atmospheric conditions of our RILEWS based on logistic identifiers and the performance in identifying RIL correctly in areas with complex topography.

4.1 Atmospheric modelling

The uncertainty of precipitations is a critical factor for RILEWS (Guzzetti et al., 2019; Chikalamo et al., 2020). The uncorrected precipitation simulation showed (~0.26-0.49) to medium (~0.32-0.67) correlation values (Pearson and Spearman) in comparison to in-situ weather stations. Our results showed a spatial dependence of the precipitation error between the mesoscale model and weather station. Stations located in the SW and NW extremes of the domain presented low correlations in comparison to the WRF model (Figure 3). Moreover, the meteorological stations in the eastern zone had RMSE between 16.33 up to 18.00 mm respectively. The RMSE for the rest of the stations ranged between 8.79 and 12.24 mm. Meanwhile, MAE showed similar values for all the stations (3.44-6.67 mm), while the bias varies between -4.0 up to 5.2 mm, except in the stations on the W and SE borders (Figure 4). Therefore, our results showed that the atmospheric model did not represent the distribution spatial and temporal of the precipitation.

The corrected precipitation model showed higher performance in RMSE, correlation and bias than in the original simulations (Figure 3). The methods of the perfect prog (PP) family gave better performance than bias correction (BC) methods. The PP_M4a method generated smaller errors in the corrected fields compared to meteorological stations. The best-performing BC method, gpQM, did not diminish the MAE, which increased by 0.05 mm on average over the uncorrected model, but it

180 did improve the RMSE by 2.47 mm on average (Figure 3). Finally, the Spearman correlation produced a lower correspondence with the observations than did the uncorrected simulation. Therefore, our results showed that the mesoscale correction allows improving the rainfall representation quality.

Figure 3 Precision and Reliability Indicators. Bias (mm), MAE (mm), RMSE (mm) and Spearman. WRF is the uncorrected model, while the other models are the different methodologies used for correction by Meteolab.

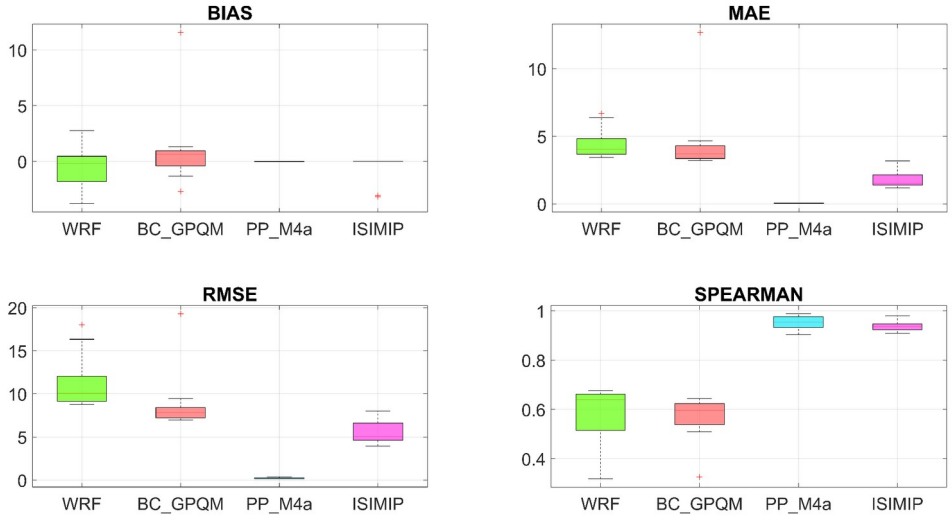

185

Figure 4 Spatial distribution of model corrected at weather stations using best results (PP_M4a). a) BIAS of the simulation in comparison with stations; b) MAE of the simulation in comparison with stations; c) RMSE of the simulation in comparison with stations; d) Spearman of the simulation in comparison with stations. Hillshade based on SRTM data.

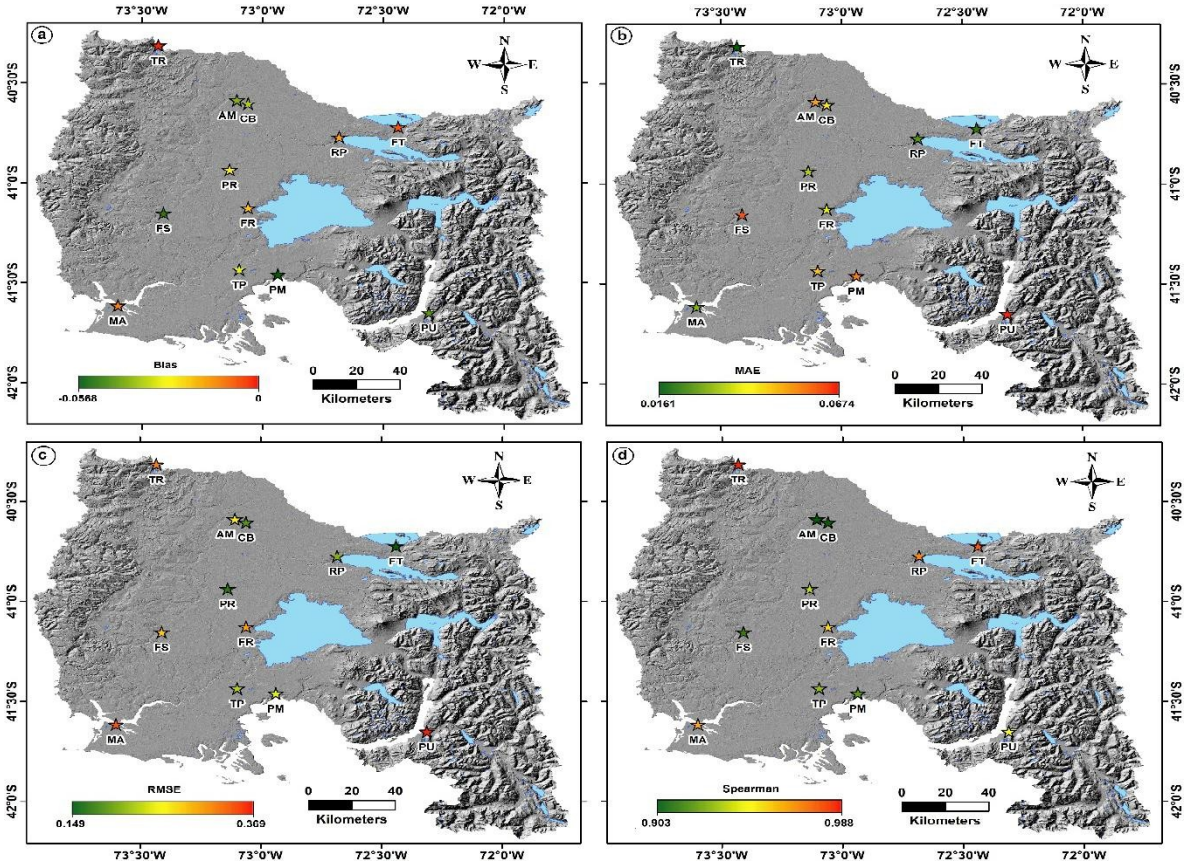

The precipitation fields corrected with different approaches of MeteoLab (Table 2) showed improved values in weather stations in comparison to raw solution. The corrected ISI-MIP results were similar to those described for PP_M4a, but with slightly larger error values. Both ISI-MIP and PP_M4a presented a bias lower than 0.5 mm. The gpQM method varied between -2.69 and 0.95 mm (Figure 3). We point out that the PP_M4a method shown the best performance considering MAE and the RMSE (~0.04 and ~0.23 mm respectively). The Spearman coefficient ranged between 0.90 and 0.98, increasing the quality of representation of the precipitation fields in comparison to weather stations.

4.2 Rainfall-Induced Landslide Early warning

The probability of occurrence of RIL at spatial and temporal scale was estimated using the precipitation values corrected on PP_M4a approach (Table 2). The results of the Logit regression (Table XXX1) showed that the weight of the intercept varied by a maximum of ~0.36 units for the 4 models, varying between 3.1658 ± 0.0091 and 3.5235 ± 0.0069 (Figure 5). The β_k' estimators corresponding to the daily precipitation fluctuated between -0.8176 ± 0.0089 and -0.8124 ± 0.0066 [1/mm],

while for the precipitation of the previous 7 days the estimator varied from -0.6413 ± 0.0063 to 0.0020 ± 0.0086 [1/mm]. The indicator obtained for the monthly precipitation was -0.3518 ± 0.0033 [1/mm] (used exclusively for the M3 model), while the slope estimator fluctuated between -0.1696 ± 0.0049 and -1289 ± 0.0072 [1/degree] (Figure 5).

TABLE XXX1: Values of the estimators for the Logit models

	Intercept	**Daily precipitation**	**Seven-day accumulated precipitation**	**Thirty-day accumulated precipitation**	**Slope**
Model 1	3.5235 ± 0.0069	- 0.8176 ± 0.0089	-	-	-0.1696 ± 0.0049
Model 2	3.3582±0.0067	-	0.6413 ± 0.0063	-	0.1365 ± 0.0086
Model 3	3.1658±0.0091	-	-	0.3518 ± 0.0033	-0.1289 ± 0.0072
Model 4	3.5206±0.0106	- 0.8124 ± 0.0066	0.0020 ± 0.0086	-	-0.1675 ± 0.0080

TABLE XXX2: Values of the estimators for the Probit models

	Intercept	**Daily precipitation**	**Seven-day accumulated precipitation**	**Thirty-day accumulated precipitation**	**Slope**
Model 1	1.9113 ± 0.0030	- 0.4166 ± 0.0046	-	-	- 0.0741 ± 0.0022
Model 2	1.8490±0.0031	-	-0.3545±0.0029	-	-0.0675 ± 0.0038
Model 3	1.7482±0.0041	-	-	-0.1897±.0020	- 0.0596±0.0033
Model 4	1.9110±0.0044	- 0.4016±0.0027	- 0.0202±0.0038	-	- 0.0732±0.0040

We point out that estimators related to the precipitation had a higher absolute weight than the slope for all the models calibrated. The precipitation used in daily (M1), previous 7 days (M2) or previous 30 days (M3) showed a decreasing value (in absolute terms) as the accumulated precipitation period increased. The results of the PP_M4a model, which considered the daily precipitation in conjunction with that of the previous 7 days, showed that the latter had an absolute weight of almost zero compared to the former. In general, the standard deviations ($\sigma_k^{\square}$) obtained from the estimators and intercept were very low for all the Logit models calibrated. The Probit model (Table XXX2) showed the same behaviour (as the Logit) of the intercept for the 4 models; its estimator fluctuated between 1.7482 ± 0.0041 and 1.9113 ± 0.0030. The β_k values for daily

precipitation varied from -0.4166 ± 0.0046 to -0.4016 ± 0.0027; 7-day precipitation from -0.3545 ± 0.0029 to -0.0202 ± 0.0038; 30-day precipitation with -0.1897 ± 0.0020 (just used in M3), and the slope from -0.0741 ± 0.0022 to -0.0596 ± 0.0033 (Figure 6).

225

Figure 5 Distribution of estimators for each model with Logit distribution.

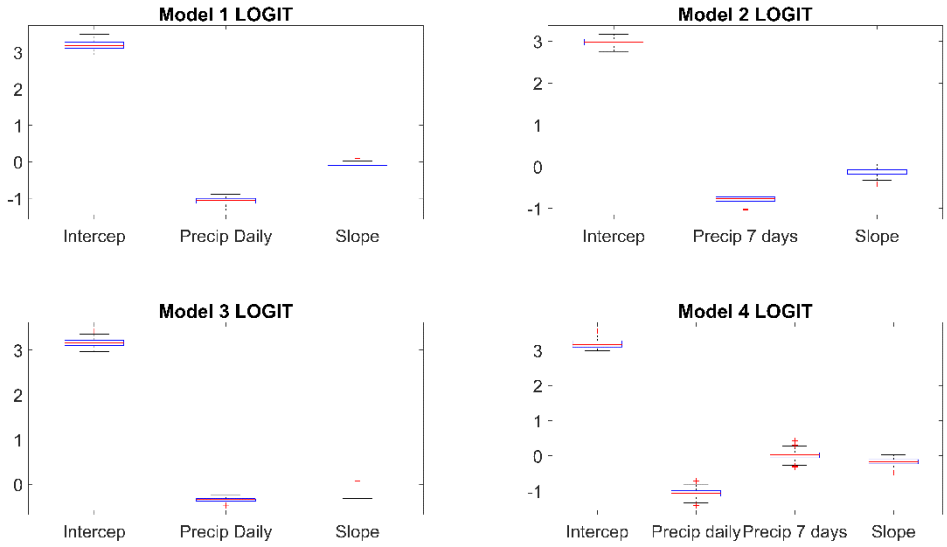

Figure 6 Distribution of estimators for each model with Probit distribution.

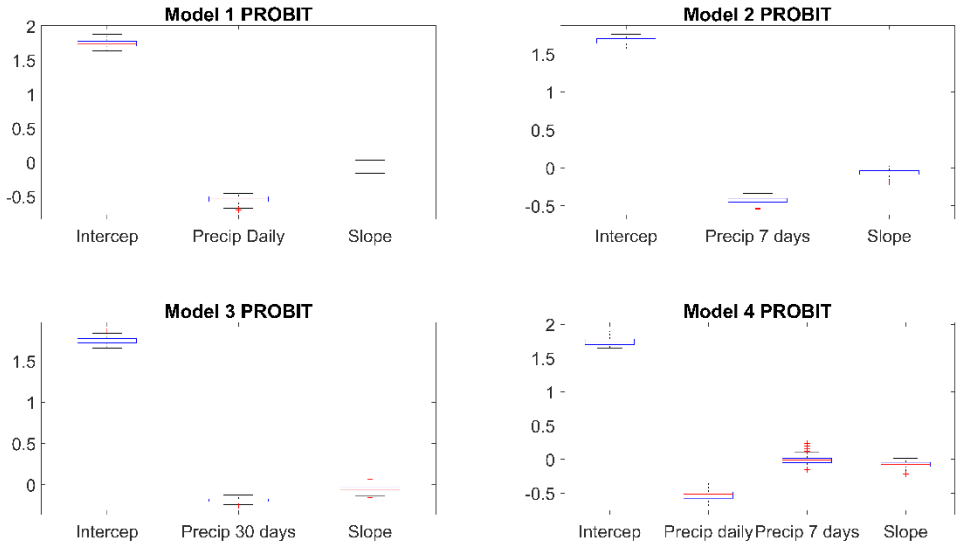

4.3 Performance assessment

ROC analysis of the Logit and Probit models showed that the M1, M2 and M4 models gave a similar performance (Figure 7 and Figure 8). The area under the curve for the Logit models varied between 0.8032 and 0.6672, while for the Probit models it varied between 0.8076 and 0.6672. Our results showed a lack of performance for M3 in comparison to daily precipitation data for Logit and Probit models (0.6582 and 0.6672, respectively). Models with AUC values equal to 0.5 indicate that do not suitable of discriminate the landslides, generating random predictions. Therefore, our results demonstrate that the calibrated models do not do a random fitting.

The rate of valid positives in the Logit distributions of the M1 and M4 models was higher than 0.97 with tolerances below 50%. For the same range, however, the rate of FP was over 45%. The same occurred with the Probit models. For a tolerance of 95%, the prediction of FN for both regressions diminished to below 40%, although the accurate predictions (TP) also fell by ~11%. Similar performance was observed in M2, with slightly higher numbers of FP, but fewer as a proportion of TP. M3 in contrast presented rates of accurate predictions and FN close to 1 for thresholds lower than 85%. In general, we observe that the Probit models had greater AUC values than the Logit being more suitable for RILEWS.

Figure 7 **ROC curve for thresholds of 5 to 99% for Logit models.**

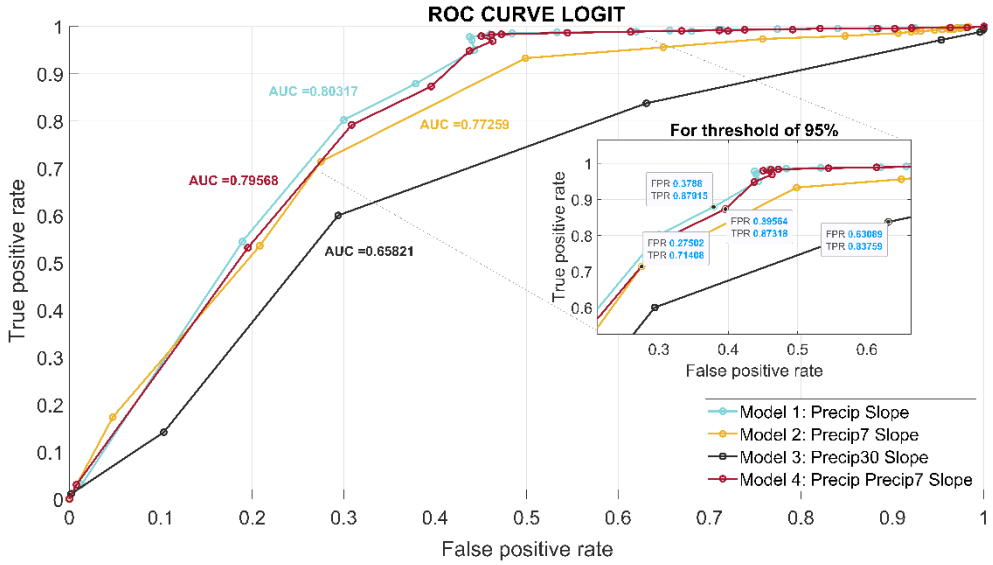

245

Figure 8 ROC curve for thresholds of 5 to 99% for Probit models.

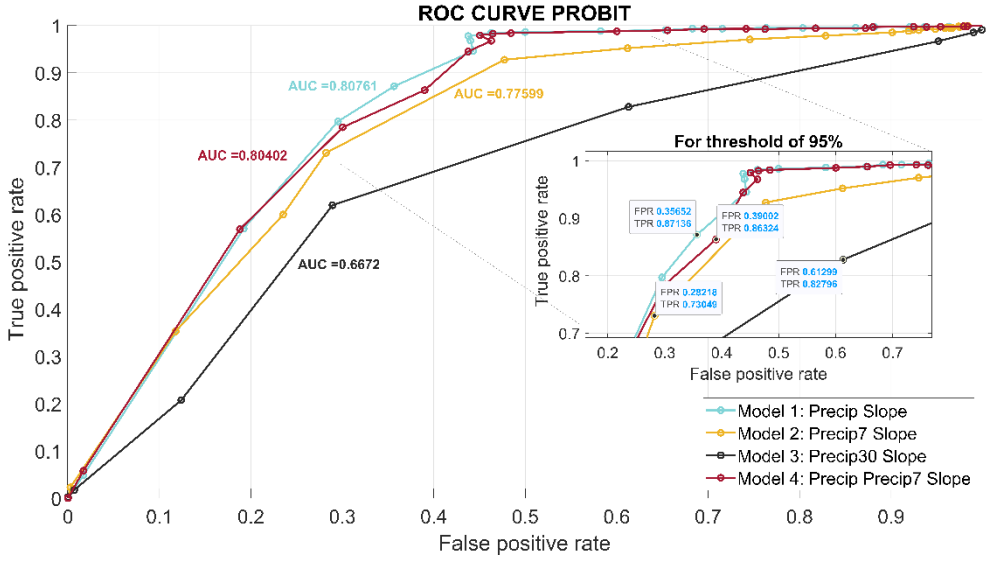

The Logit and Probit regressions for M1 and M4 presented the highest sensitivity values, of 91.79 ± 1.95% and 91.81 ± 2.00% respectively, for the Logit regressions (Table 3). In the Probit models, M1 and M4 achieved sensitivity values of 250 91.25 ± 1.96% and 91.16 ± 2.03% respectively. Likewise, M2 had a sensitivity of 87.07 ± 2.93% for Logit and 86.19 ±

2.79% for Probit. The sensitivity of M3 was 83.89 ± 5.46% for Logit and 82.94 ± 5.21 for Probit (Table 3). In general, we observed that the Logit models were more sensitive than the Probit. The specificity values for the M2 and M3 models were subtly higher for the Probit regressions than for the Logit, while for the M1 and M4 models the results obtained were almost equal.

Table 3: Sensitivity and specificity with validation database (BD2).

Model	Distribution	Sensitivity (%)	Specificity (%)
Model 1	Logit	91.79 ± 1.95	54.36 ± 14.11
	Probit	91.25 ± 1.96	54.29 ± 14.11
Model 2	Logit	87.07 ± 2.93	62.43 ± 14.29
	Probit	86.19 ± 2.79	64.18 ± 14.03
Model 3	Logit	83.89 ± 5.46	36.11 ± 16.41
	Probit	82.94 ± 5.21	38.18 ± 16.44
Model 4	Logit	91.81 ± 2.00	55.65 ± 14.46
	Probit	91.16 ± 2.03	55.71 ± 14.49

According to this, the best model for predicting RIL in the study area was M1 (daily precipitation and slope). The sensitivity and specificity values with the 95% threshold chosen after ROC analysis were higher than 82%. The results showed that the indicators were similar for the M1, M3 and M4 models (Table 3). However, a reduction was observed in the rate of TP for the M2 model (~10%).

5 Analysis and Discussion

Implementing RILEWS is a challenge due to the natural limitations like historical records and the precipitation data available. One of the main challenges in RILEWS corresponds to develop a model that generates warning only using limited meteorological information. Therefore, precipitation representation characterized by a low uncertainty in complex topography environments is a valuable contribution (Table 3). Our study proposes an alternative to landslide forecast into scarce data environments, allowing to increase the resilience of the local community. Here, we demonstrated that the mesoscale models become suitable to reproduce the spatial precipitation distribution with a bias-correct using in-situ weather stations. The precipitation was integrated into a logistic model subsequently, to establish the spatial probability of occurrence of a RIL event.

5.1 Atmospheric modelling

Implementation of a LEWS applied to RIL requires accurate estimation of the spatial distribution of precipitation. Zones with a low density of meteorological stations generate uncertainties in the RILEWS implementation (Marra, 2018; Peres et al., 2018). Previous works have shown the sensitivity of mesoscale models to abrupt changes of complex topography (Srivastava et al., 2015; Osman et al., 2018; Heredia et al., 2018; Jeong & Lee, 2018; Buchici et al., 2019; Bannister et al., 2019; Worku et al., 2020); being consistent with the abrupt topography of the eastern part of the study area (Figure 4), where the MAE (6.6) and RMSE (17.9) values were concentrated. We avoided the precipitation constrain using a bias-corrected version of the WRF model to reduce the spatial error estimation in the precipitations. The use of bias-corrected precipitation of the WRF model improved the spatial representation in this study. The uncorrected model had bias values higher than 16 mm, becoming critical during the incorrect early warning generation. Therefore, an incorrect precipitation estimation could becomes a human loss. Following, our results deliver precipitation data with a low uncertainty level. That becomes suitable to operative RILEWS with a low false-positive rate (FP).

In many areas of the world, the prediction of rainfall-induced landslides is usually carried out using empirical rainfall thresholds [Gariano et al., 2020]. Previous contributions showed that dense weather stations allow representing the complex precipitation distribution giving well threshold estimation [Nikolopoulos et al., 2014]. However, debris flow thresholds developed from sparse in-situ weather stations generated low performance [Nikolopoulos et al., 2015]. The complex topography and the sparse weather stations availability underestimate rainfall thresholds for landslides in Southern Andes. Following, a RILEWS based only on weather stations is not suitable. Previous studies showed a systematic underestimation in debris flow early warning thresholds related to the use of sparse rain gauge networks [Marra et al., 2016; Destro et al., 2017; Marra et al., 2017]. Moreover, the topography has a strong influence on modifying the spatial distribution of precipitation that leads to debris flows [Marra et al., 2016; Fustos et al., 2021] and landslides [Fustos et al., 2017]. Hence, our contribution allows reducing the precipitation estimation uncertainty increasing the reliability of RILEWS in the Southern Andes.

From our results, the bias-correction improved the precipitation representation when we compared against the weather stations (Figure 4). The data from 12 spatially distributed meteorological stations were sufficient to represent the precipitation fields with low RMSE values (max. 0.36 mm). Thus, the corrected results represent the precipitation fields in Andean areas with lower bias values than previous studies (Yáñez-Morroni et al., 2018; Schumacher et al., 2020). PP_M4a approach was found to reduce the bias efficiently for the study area. We propose that perfect prog approach allow to represent accurately the topographic influence in the precipitation if the distribution of the weather stations is available. We note that 30% of all the RIL occurred on days with low precipitation on the day and during the preceding days (7 and 30 days previous). Therefore, we propose that future developments should progress to analysis on a sub-daily scale. In this

context, future developments should aim to use corrected WRF at an hourly scale; or else use lower-resolution satellite estimates of precipitation as a tool to complement WRF simulations.

5.2 Rainfall-Induced Landslide Early Warning

The Southern Andes has a complex topography that influences precipitation events with different intensities in a few kilometres of separation (examples in Figure 9 and Figure 10). Hence, a correct precipitation representation along the space allows increasing the sensibility. The sensitivity of RILEWS depends heavily on the input variables, specifically the precipitation in this case. The RILEWS achieved high predictive ability with AUC values between 0.65 (M3) and 0.80 (M1), suggesting high sensitivity to intense precipitations in short periods. The performance of the model diminished when data at monthly scale were used (M3) in comparison with daily resolution (M1 and M2), where M2 model (AUC=0.77) had similar performance to M1. This similarity may be associated with the soil moisture content, reflecting the previous precipitation; this means that it functions as a memory of the soil moisture in the slope before a RIL (related to the different soil types). The memory effect in the slope in M3 will reflect in part its predisposition to suffer a RIL based on the soil moisture content in the first few centimetres. Numerous works have related satellite information on precipitation and soil moisture to establish links between them (Brocca et al., 2020; Camici et al., 2020; Pellarin et al., 2020). In future, the soil moisture memory approach could be the best way to obtain a proxy of the soil moisture content and the slope response to landslides in zones without a network of moisture sensors. This is consistent when we compare M1 (AUC=0.80) and M4 (AUC=0.79); they present similar sensitivity values (~91% in both cases), suggesting that either model could be used. Model 1 and Model 4 showed similar performance because one being contained in the second. Hence, we interpret that an overrepresentation could exist. Therefore, model 4 does not support additional information. At an operational level, the discard of model 4 reduces the computing loading, simplifying the alert processes.

Figure 9 Zones susceptible to RIL for January 08, 2017. Results using Model 1 (logit). Hillshade based on SRTM data.

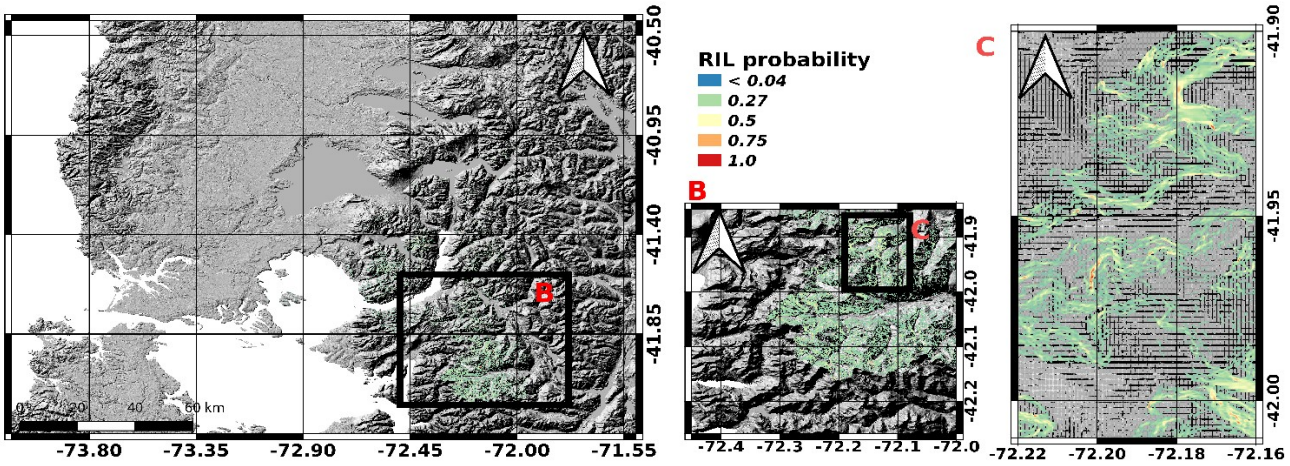

325 **Figure 10 Zones susceptible to RIL for January 08, 2017. Results using Model 1 (probit).**

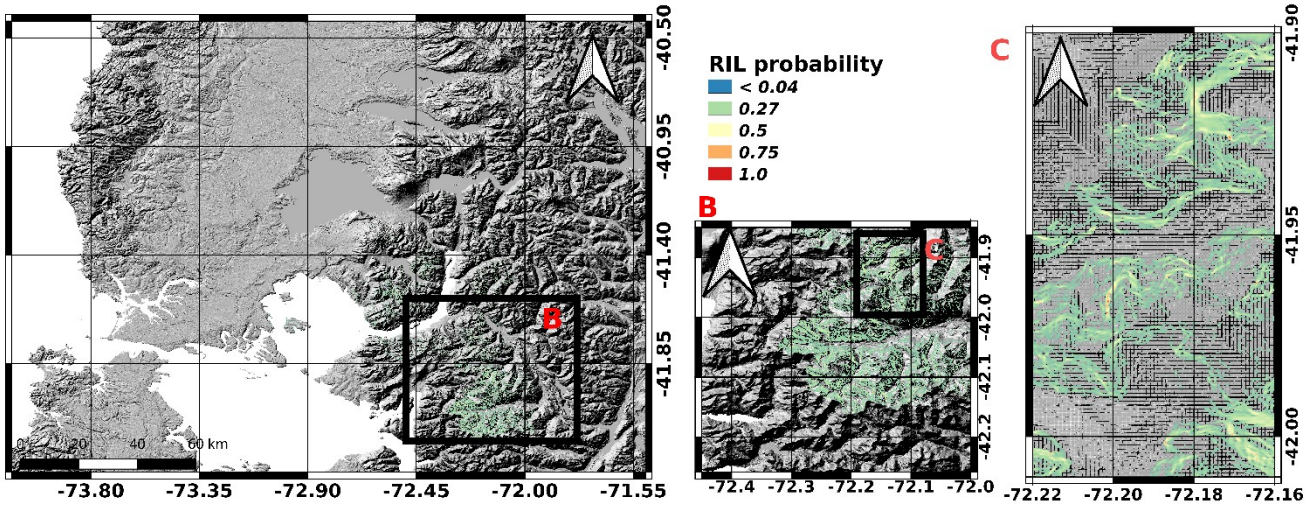

5.3 Future developments

The Andes in one of the most susceptible zones to be affected by intense precipitation changes product of climate change.
330 To reproduce and understand intense precipitation changes and their impact on landslides, a high Spatio-temporal resolution is needed. The present contribution support reproducing accurate precipitation, contributing to robust RILEWS. Potential improvements should be directed towards increasing the predictive ability by increasing the temporal resolution of the

precipitation products. Our models do not consider the soil hydraulic variability like tephra fall or intensely weathered soft rocks. Recently, rainfall-induced landslides affected actives (Fustos et al., 2021) and older volcanic environments (Somos et al., 2020). The new generation of RILEWS will need a parametrization of these environments from a geotechnical point of view. Moreover, all RILEWS must be able to be automated, which involves computing capacities of various kinds; to mitigate the calculation costs we suggest incorporating the available satellite precipitation products, but at lower spatial resolution (~10 km). Satellite estimations require validation of these outputs in areas with complex topography, like southern Chile (Zambrano-Bigiarini et al., 2017). Likewise, new geoscientific data interfaces like GSMaP will allow better integration with precipitation, complementing WRF products. One limitation of the present study is the quality of the RIL inventory used. South America presents a low density of recorded events, despite the high density of their occurrence. Future efforts should be directed towards generating RIL identification records using remote sensor techniques (Guzzetti et al., 2020; Fustos et al., 2017; Jia et al., 2019) or numerical identification (Chikalamo et al., 2020; Guzzetti et al., 2020; Fustos et al., 2020a). To date, our database is the best available for the spatial location and date of generation in the study area. We suggest that alternatives should be considered in future to strengthen the generation of RIL databases in the Southern Andes with a larger number of events. This could help to strengthen future RILEWS in this area, improving their performance in terms of sensitivity and specificity.

6 Conclusions

This work evaluated the implementation of a RILEWS based on a logistic model and forced by geomorphological and atmospheric conditions in the Southern Andes. For the first time in the Southern Andes, we showed how the WRF model can be integrated into RILEWS operating systems without the need to use ensembles, by use of bias correction processes. This opens the door to the implementation of precipitation-based prediction models without costly computer iterations by ensembles of models (Yáñez-Morroni et al., 2018; Schumacher et al., 2020). New studies of LEWS in the Southern Andes should be directed towards increasing the RIL database currently available. In future we suggest evaluating alternatives to strengthen better quality RIL database generation in this segment of South America, completing the existing database from the records of the Chilean National Geological and Mining Service (Sernageomin). This could help to strengthen future RILEWS in the Southern Andes, improving their performance in terms of sensitivity and specificity.

Logistic models proved their capacity to predict RIL events with AUC varying between 0.65 and 0.80, indicating their ability to represent RIL occurrence correctly. Despite the high relative sensitivity of M3, the models which presented high sensitivity and specificity were those which included precipitations on a daily scale (models 1, 2 and 4). Using the precipitation of the previous 7 days could improve this approach to representing soil moisture. There is no network of moisture sensors in the area, so Model 4 should be incorporated as it allows this factor to be represented. Finally, we propose to use models M1 and M4 in conjunction.

Acknowledgements

We acknowledge Dirección de Investigación of the University of La Frontera for their English editing support.

Author contributions

NM and IF contributed to the conceptualization and methodology of the research and performed the formal analysis, visualization, and validation. NM carried out the numerical simulations and following validations. IF, DV, VL and MH contributed with the supervision, review, and editing of the paper.

Competing interests

The authors declare that they have no conflict of interest.

Financial support

This was made possible thanks to the "Agencia Nacional de Investigación y Desarrollo (ANID)", “Fondecyt Iniciación” program (grant no. 11180500) of the Chilean government.

References

Alvarez-Garreton, C., Mendoza, P. A., Boisier, J. P., Addor, N., Galleguillos, M., Zambrano-Bigiarini, M., Lara, A., Puelma, C., Cortes, G., Garreaud, R., McPhee, J., and Ayala, A.: The CAMELS-CL dataset: catchment attributes and meteorology for large sample studies – Chile dataset, Hydrol. Earth Syst. Sci., 22, 5817–5846, https://doi.org/10.5194/hess-22-5817-2018, 2018.

Bai, S., Lu, P., and Thiebes, B.: Comparing characteristics of rainfall- and earthquake-triggered landslides in the Upper Minjiang catchment, China, Engineering Geology, 268, 105518, https://doi.org/10.1016/j.enggeo.2020.105518, 2020.

Bannister, D., Orr, A., Jain, S. K., Holman, I. P., Momblanch, A., Phillips, T., Adeloye, A. J., Snapir, B., Waine, T. W., Hosking, J. S., and Allen‐Sader, C.: Bias Correction of High‐Resolution Regional Climate Model Precipitation Output Gives the Best Estimates of Precipitation in Himalayan Catchments, J. Geophys. Res. Atmos., 124, 14220–14239, https://doi.org/10.1029/2019jd030804, 2019.

Beck, H. E., Zimmermann, N. E., McVicar, T. R., Vergopolan, N., Berg, A., and Wood, E. F.: Present and future Köppen-Geiger climate classification maps at 1-km resolution, Sci Data, 5, https://doi.org/10.1038/sdata.2018.214, 2018.

Bernard, M. and Gregoretti, C.: The Use of Rain Gauge Measurements and Radar Data for the Model‐Based Prediction of Runoff‐Generated Debris‐Flow Occurrence in Early Warning Systems, Water Res, 57, https://doi.org/10.1029/2020wr027893, 2021.

Blanco, D. E. and de la Balze, V. M.: Los Turbales de la Patagonia. Bases para su inventario y la conservación de su biodiversidad, Wetl. Int., 19, 2004.Brocca, L., Massari, C., Pellarin, T., Filippucci, P., Ciabatta, L., Camici, S., Kerr, Y. H., and Fernández-Prieto, D.: River flow prediction in data scarce regions: soil moisture integrated satellite rainfall products outperform rain gauge observations in West Africa, Sci Rep, 10, https://doi.org/10.1038/s41598-020-69343-x, 2020.

Camici, S., Massari, C., Ciabatta, L., Marchesini, I., and Brocca, L.: Which rainfall score is more informative about the performance in river discharge simulation? A comprehensive assessment on 1318 basins over Europe, Hydrol. Earth Syst. Sci., 24, 4869–4885, https://doi.org/10.5194/hess-24-4869-2020, 2020.

Chapanov, Y., Atanasova, M. and Nikolov, H.: Heavy rainfalls in Bulgaria due to solar activity and their possible influence on landslides, in 10th Congress of Balkan Geophysical Society, BGS 2019., 2019.

Chikalamo, E. E., Mavrouli, O. C., Ettema, J., van Westen, C. J., Muntohar, A. S., and Mustofa, A.: Satellite-derived rainfall thresholds for landslide early warning in Bogowonto Catchment, Central Java, Indonesia, International Journal of Applied Earth Observation and Geoinformation, 89, 102093, https://doi.org/10.1016/j.jag.2020.102093, 2020.

Cremonini, R. and Tiranti, D.: The Weather Radar Observations Applied to Shallow Landslides Prediction: A Case Study From North-Western Italy, Front. Earth Sci., 6, https://doi.org/10.3389/feart.2018.00134, 2018.

Destro, E., Marra, F., Nikolopoulos, E. I., Zoccatelli, D., Creutin, J. D., and Borga, M.: Spatial estimation of debris flows-triggering rainfall and its dependence on rainfall return period, Geomorphology, 278, 269–279, https://doi.org/10.1016/j.geomorph.2016.11.019, 2017.

Fan, X., Xu, Q., Liu, J., Subramanian, S. S., He, C., Zhu, X., and Zhou, L.: Successful early warning and emergency response of a disastrous rockslide in Guizhou province, China, Landslides, 16, 2445–2457, https://doi.org/10.1007/s10346-019-01269-6, 2019.

Fawcett, T.: ScienceDirect.com - Pattern Recognition Letters - An introduction to ROC analysis, Pattern Recognit. Lett., 27(8), 2006.

Froude, M. J. and Petley, D. N.: Global fatal landslide occurrence from 2004 to 2016, Nat. Hazards Earth Syst. Sci., 18, 2161–2181, https://doi.org/10.5194/nhess-18-2161-2018, 2018. a, b, c

Fustos, I., Abarca-del-Rio, R., Ávila, A., and Orrego, R.: A simple logistic model to understand the occurrence of flood events into the Biobío River Basin in central Chile, J Flood Risk Management, 10, 17–29, https://doi.org/10.1111/jfr3.12131, 2014.

Fustos, I., Abarca-del-Río, R., Mardones, M., González, L., and Araya, L. R.: Rainfall-induced landslide identification using numerical modelling: A southern Chile case, Journal of South American Earth Sciences, 101, 102587, https://doi.org/10.1016/j.jsames.2020.102587, 2020.

Fustos, I., Abarca-del-Rio, R., Moreno-Yaeger, P., and Somos-Valenzuela, M.: Rainfall-Induced Landslides forecast using local precipitation and global climate indexes, Nat Hazards, 102, 115–131, https://doi.org/10.1007/s11069-020-03913-0, 2020.

Fustos-Toribio, I. J., Morales-Vargas, B., Somos-Valenzuela, M., Moreno-Yaeger, P., Muñoz-Ramirez, R., Rodriguez Araneda, I., and Chen, N.: Debris Flow event on Osorno volcano, Chile, during summer 2017: New interpretations for chain processes in the Southern Andes, Nat. Hazards Earth Syst. Sci. https://doi.org/10.5194/nhess-2021-74, 2021.

Gariano, S. L. and Guzzetti, F.: Landslides in a changing climate, Earth-Science Reviews, 162, 227–252, https://doi.org/10.1016/j.earscirev.2016.08.011, 2016.

Gariano, S. L., Melillo, M., Peruccacci, S. et al. How much does the rainfall temporal resolution affect rainfall thresholds for landslide triggering?. Nat Hazards, 100, 655–670. https://doi.org/10.1007/s11069-019-03830-x, 2020

Gomez-Cardenas, P. and Garrido-Urzua, N.: Catastro de remociones en masa en la región de Los Lagos, Chile. XV Congreso Geológico Chileno, November 16, Concepción-Chile. Article available at: https://congresogeologicochileno.cl/wp-content/uploads/2018/12/Libro-de-Actas-XVCongresoGeologicoChileno2018-2.pdf, . 2018.

Gutjahr, O. and Heinemann, G.: Comparing precipitation bias correction methods for high-resolution regional climate simulations using COSMO-CLM, Theor Appl Climatol, 114, 511–529, https://doi.org/10.1007/s00704-013-0834-z, 2013.

Guzzetti, F., Gariano, S. L., Peruccacci, S., Brunetti, M. T., Marchesini, I., Rossi, M., and Melillo, M.: Geographical landslide early warning systems, Earth-Science Reviews, 200, 102973, https://doi.org/10.1016/j.earscirev.2019.102973, 2020.

Hand, D. J. and Till, R. J.: A Simple Generalisation of the Area Under the ROC Curve for Multiple Class Classification Problems, Mach. Learn., 45(2), https://doi.org/10.1023/A:1010920819831, 2001.

Hempel, S., Frieler, K., Warszawski, L., Schewe, J., and Piontek, F.: A trend-preserving bias correction – the ISI-MIP approach, Earth Syst. Dynam., 4, 219–236, https://doi.org/10.5194/esd-4-219-2013, 2013.

Hermle, D., Keuschnig, M., Hartmeyer, I., Delleske, R., and Krautblatter, M.: Timely prediction potential of landslide early warning systems with multispectral remote sensing: a conceptual approach tested in the Sattelkar, Austria, Nat. Hazards Earth Syst. Sci., 21, 2753–2772, https://doi.org/10.5194/nhess-21-2753-2021, 2021

Heredia, M. B., Junquas, C., Prieur, C. and Condom, T.: New statistical methods for precipitation bias correction applied to WRF model simulations in the Antisana Region, Ecuador, J. Hydrometeorol., 19(12), doi:10.1175/JHM-D-18-0032.1, 2018.

Hong, S. Y., Dudhia, J. and Chen, S. H.: A revised approach to ice microphysical processes for the bulk parameterization of clouds and precipitation, Mon. Weather Rev., 132(1), https://doi.org/10.1175/1520-0493(2004)132<0103:ARATIM>2.0.CO;2, 2004.

Jeong, J. and Lee, S.-J.: A Statistical Parameter Correction Technique for WRF Medium-Range Prediction of Near-Surface Temperature and Wind Speed Using Generalized Linear Model, Atmosphere, 9, 291, https://doi.org/10.3390/atmos9080291, 2018.

Jia, H., Zhang, H., Liu, L., and Liu, G.: Landslide Deformation Monitoring by Adaptive Distributed Scatterer Interferometric Synthetic Aperture Radar, Remote Sensing, 11, 2273, https://doi.org/10.3390/rs11192273, 2019.

Kirschbaum, D. B., Adler, R., Hong, Y., Hill, S., and Lerner-Lam, A.: A global landslide catalog for hazard applications: method, results, and limitations, Nat. Hazards, 52, 561–575, 2010. a, b

Lazzari, M. and Piccarreta, M.: Landslide Disasters Triggered by Extreme Rainfall Events: The Case of Montescaglioso (Basilicata, Southern Italy), Geosciences, 8, 377, https://doi.org/10.3390/geosciences8100377, 2018.

Lee, W. Y., Park, S. K., and Sung, H. H.: The optimal rainfall thresholds and probabilistic rainfall conditions for a landslide early warning system for Chuncheon, Republic of Korea, Landslides, 18, 1721–1739, https://doi.org/10.1007/s10346-020-01603-3, 2021.

Li, H., Lee, Y.-C., Zhou, Y.-C., and Sun, J.: The random subspace binary logit (RSBL) model for bankruptcy prediction, Knowledge-Based Systems, 24, 1380–1388, https://doi.org/10.1016/j.knosys.2011.06.015, 2011.

Marjanović, M., Krautblatter, M., Abolmasov, B., Đurić, U., Sandić, C., and Nikolić, V.: The rainfall-induced landsliding in Western Serbia: A temporal prediction approach using Decision Tree technique, Engineering Geology, 232, 147–159, https://doi.org/10.1016/j.enggeo.2017.11.021, 2018.

Marra, F., Nikolopoulos, E. I., Creutin, J. D., and Borga, M.: Space–time organization of debris flows-triggering rainfall and its effect on the identification of the rainfall threshold relationship, Journal of Hydrology, 541, 246–255, https://doi.org/10.1016/j.jhydrol.2015.10.010, 2016.

Marra, F.: Rainfall thresholds for landslide occurrence: systematic underestimation using coarse temporal resolution data, Nat Hazards, 95, 883–890, https://doi.org/10.1007/s11069-018-3508-4, 2018.

Marra, F., Destro, E., Nikolopoulos, E. I., Zoccatelli, D., Creutin, J. D., Guzzetti, F., and Borga, M.: Impact of rainfall spatial aggregation on the identification of debris flow occurrence thresholds, Hydrol. Earth Syst. Sci., 21, 4525–4532, https://doi.org/10.5194/hess-21-4525-2017, 2017.

National Centers For Environmental Prediction/National Weather Service/NOAA/U.S. Department Of Commerce: NCEP FNL Operational Model Global Tropospheric Analyses, continuing from July 1999, https://doi.org/10.5065/D6M043C6, 2000.

Nikolopoulos, E. I., Crema, S., Marchi, L., Marra, F., Guzzetti, F., and Borga, M.: Impact of uncertainty in rainfall estimation on the identification of rainfall thresholds for debris flow occurrence, Geomorphology, 221, 286–297, https://doi.org/10.1016/j.geomorph.2014.06.015, 2014.

Nikolopoulos, E. I., Borga, M., Creutin, J. D., and Marra, F.: Estimation of debris flow triggering rainfall: Influence of rain gauge density and interpolation methods, Geomorphology, 243, 40–50, https://doi.org/10.1016/j.geomorph.2015.04.028, 2015.

Osman, M., Zittis, G., AbouElHaggag, M., Abdeldayem, A. and Lelieveld, J.: Optimizing WRF as a regional climate Downscaling Tool for Hydro-climatological Applications in the Eastern Nile Basin, , www.doi.org/10.31223/OSF.IO/FX7AW, 2019.

Pellarin, T., Román-Cascón, C., Baron, C., Bindlish, R., Brocca, L., Camberlin, P., Fernández-Prieto, D., Kerr, Y. H., Massari, C., Panthou, G., Perrimond, B., Philippon, N., and Quantin, G.: The Precipitation Inferred from Soil Moisture (PrISM) Near Real-Time Rainfall Product: Evaluation and Comparison, Remote Sensing, 12, 481, https://doi.org/10.3390/rs12030481, 2020.

Peres, D. J. and Cancelliere, A.: Derivation and evaluation of landslide-triggering thresholds by a Monte Carlo approach, Hydrol. Earth Syst. Sci., 18, 4913–4931, https://doi.org/10.5194/hess-18-4913-2014, 2014.

Peres, D. J. and Cancelliere, A.: Comparing methods for determining landslide early warning thresholds: potential use of non-triggering rainfall for locations with scarce landslide data availability, Landslides, 18, 3135–3147, https://doi.org/10.1007/s10346-021-01704-7, 2021.

Peres, D. J., Cancelliere, A., Greco, R., and Bogaard, T. A.: Influence of uncertain identification of triggering rainfall on the assessment of landslide early warning thresholds, Nat. Hazards Earth Syst. Sci., 18, 633–646, https://doi.org/10.5194/nhess-18-633-2018, 2018.

Peruccacci, S., Brunetti, M. T., Gariano, S. L., Melillo, M., Rossi, M., and Guzzetti, F.: Rainfall thresholds for possible landslide occurrence in Italy, Geomorphology, 290, 39–57, https://doi.org/10.1016/j.geomorph.2017.03.031, 2017.

Tavakkoli Piralilou, S., Shahabi, H., Jarihani, B., Ghorbanzadeh, O., Blaschke, T., Gholamnia, K., Meena, S., and Aryal, J.: Landslide Detection Using Multi-Scale Image Segmentation and Different Machine Learning Models in the Higher Himalayas, Remote Sensing, 11, 2575, https://doi.org/10.3390/rs11212575, 2019.

De Reu, J., Bourgeois, J., Bats, M., Zwertvaegher, A., Gelorini, V., De Smedt, P., Chu, W., Antrop, M., De Maeyer, P., Finke, P., Van Meirvenne, M., Verniers, J., and Crombé, P.: Application of the topographic position index to heterogeneous landscapes, Geomorphology, 186, 39–49, https://doi.org/10.1016/j.geomorph.2012.12.015, 2013.

Rossi, M., Luciani, S., Valigi, D., Kirschbaum, D., Brunetti, M. T., Peruccacci, S., and Guzzetti, F.: Statistical approaches for the definition of landslide rainfall thresholds and their uncertainty using rain gauge and satellite data, Geomorphology, 285, 16–27, https://doi.org/10.1016/j.geomorph.2017.02.001, 2017.

San-Martín, D., Manzanas, R., Brands, S., Herrera, S., and Gutiérrez, J. M.: Reassessing Model Uncertainty for Regional Projections of Precipitation with an Ensemble of Statistical Downscaling Methods, J. Climate, 30, 203–223, https://doi.org/10.1175/jcli-d-16-0366.1, 2017.

Sarma, C. P., Dey, A., and Krishna, A. M.: Influence of digital elevation models on the simulation of rainfall-induced landslides in the hillslopes of Guwahati, India, Engineering Geology, 268, 105523, https://doi.org/10.1016/j.enggeo.2020.105523, 2020.

Sättele, M., Bründl, M., and Straub, D.: Reliability and effectiveness of early warning systems for natural hazards: Concept and application to debris flow warning, Reliability Engineering & System Safety, 142, 192–202, https://doi.org/10.1016/j.ress.2015.05.003, 2015.

Schumacher, V., Fernández, A., Justino, F., and Comin, A.: WRF High Resolution Dynamical Downscaling of Precipitation for the Central Andes of Chile and Argentina, Front. Earth Sci., 8, https://doi.org/10.3389/feart.2020.00328, 2020.

Sepúlveda, S. A. and Petley, D. N.: Regional trends and controlling factors of fatal landslides in Latin America and the Caribbean, Nat. Hazards Earth Syst. Sci., 15, 1821–1833, https://doi.org/10.5194/nhess-15-1821-2015, 2015.

Segoni, S., Piciullo, L., and Gariano, S. L.: Preface: Landslide early warning systems: monitoring systems, rainfall thresholds, warning models, performance evaluation and risk perception, Nat. Hazards Earth Syst. Sci., 18, 3179–3186, https://doi.org/10.5194/nhess-18-3179-2018, 2018.

Skamarock, W. C., Klemp, J. B., Dudhia, J., Gill, D. O., Liu, Z., Berner, J., Wang, W., Powers, J. G., Duda, M. G., Barker, D. M., and Huang, X.-Y.: A Description of the Advanced Research WRF Model Version 4, UCAR/NCAR, https://doi.org/10.5065/1DFH-6P97, 2019.

Srivastava, P. K., Islam, T., Gupta, M., Petropoulos, G., and Dai, Q.: WRF Dynamical Downscaling and Bias Correction Schemes for NCEP Estimated Hydro-Meteorological Variables, Water Resour Manage, 29, 2267–2284, https://doi.org/10.1007/s11269-015-0940-z, 2015.

Tewari, M., Chen, F., Wang, W., Dudhia, J., LeMone, M. A., Mitchell, K., Ek, M., Gayno, G., Wegiel, J. and Cuenca, R. H.: Implementation and verification of the unified noah land surface model in the WRF model, in Bulletin of the American Meteorological Society., 2004.

Thirugnanam, H., Ramesh, M. V., and Rangan, V. P.: Enhancing the reliability of landslide early warning systems by machine learning, Landslides, 17, 2231–2246, https://doi.org/10.1007/s10346-020-01453-z, 2020.

Tichavský, R., Ballesteros-Cánovas, J. A., Šilhán, K., Tolasz, R., and Stoffel, M.: Dry Spells and Extreme Precipitation are The Main Trigger of Landslides in Central Europe, Sci Rep, 9, https://doi.org/10.1038/s41598-019-51148-2, 2019.

Tiranti, D., Cremonini, R., Marco, F., Gaeta, A. R., and Barbero, S.: The DEFENSE (debris Flows triggEred by storms – nowcasting system): An early warning system for torrential processes by radar storm tracking using a Geographic Information System (GIS), Computers & Geosciences, 70, 96–109, https://doi.org/10.1016/j.cageo.2014.05.004, 2014.

Tiranti, D., Nicolò, G., and Gaeta, A. R.: Shallow landslides predisposing and triggering factors in developing a regional early warning system, Landslides, 16, 235–251, https://doi.org/10.1007/s10346-018-1096-8, 2018.

Wayand, N. E., Hamlet, A. F., Hughes, M., Feld, S. I., and Lundquist, J. D.: Intercomparison of Meteorological Forcing Data from Empirical and Mesoscale Model Sources in the North Fork American River Basin in Northern Sierra Nevada, California*, 14, 677–699, https://doi.org/10.1175/jhm-d-12-0102.1, 2013.

Wilcke, R. A. I., Mendlik, T., and Gobiet, A.: Multi-variable error correction of regional climate models, Climatic Change, 120, 871–887, https://doi.org/10.1007/s10584-013-0845-x, 2013.

Wang, X., Otto, M., and Scherer, D.: Atmospheric triggering conditions and climatic disposition of landslides in Kyrgyzstan and Tajikistan at the beginning of the 21st century, Nat. Hazards Earth Syst. Sci., 21, 2125–2144, https://doi.org/10.5194/nhess-21-2125-2021, 2021.

Worku, G., Teferi, E., Bantider, A., and Dile, Y. T.: Statistical bias correction of regional climate model simulations for climate change projection in the Jemma sub-basin, upper Blue Nile Basin of Ethiopia, Theor Appl Climatol, 139, 1569–1588, https://doi.org/10.1007/s00704-019-03053-x, 2019.

Yáñez-Morroni, G., Gironás, J., Caneo, M., Delgado, R., and Garreaud, R.: Using the Weather Research and Forecasting (WRF) Model for Precipitation Forecasting in an Andean Region with Complex Topography, Atmosphere, 9, 304, https://doi.org/10.3390/atmos9080304, 2018.

Yang, Q., Yu, Z., Wei, J., Yang, C., Gu, H., Xiao, M., Shang, S., Dong, N., Gao, L., Arnault, J., Laux, P., and Kunstmann, H.: Performance of the WRF model in simulating intense precipitation events over the Hanjiang River Basin, China – A multi-physics ensemble approach, Atmospheric Research, 248, 105206, https://doi.org/10.1016/j.atmosres.2020.105206, 2021.

Zambrano-Bigiarini, M., Nauditt, A., Birkel, C., Verbist, K., and Ribbe, L.: Temporal and spatial evaluation of satellite-based rainfall estimates across the complex topographical and climatic gradients of Chile, Hydrol. Earth Syst. Sci., 21, 1295–1320, https://doi.org/10.5194/hess-21-1295-2017, 2017.

Zhang, K., Xue, X., Hong, Y., Gourley, J. J., Lu, N., Wan, Z., Hong, Z., and Wooten, R.: iCRESTRIGRS: a coupled modeling system for cascading flood–landslide disaster forecasting, Hydrol. Earth Syst. Sci., 20, 5035–5048, https://doi.org/10.5194/hess-20-5035-2016, 2016.

Zhao, B., Dai, Q., Han, D., Dai, H., Mao, J., Zhuo, L., and Rong, G.: Estimation of soil moisture using modified antecedent precipitation index with application in landslide predictions, Landslides, 16, 2381–2393, https://doi.org/10.1007/s10346-019-01255-y, 2019.